



## City Research Online

### City, University of London Institutional Repository

---

**Citation:** Stanković, S. B. & Kyriacou, P. A. (2012). The effects of thermistor linearization techniques on the T-history characterization of phase change materials. *Applied Thermal Engineering*, 44(Nov), pp. 78-84. doi: 10.1016/j.applthermaleng.2012.03.032

This is the accepted version of the paper.

This version of the publication may differ from the final published version.

---

**Permanent repository link:** <https://openaccess.city.ac.uk/id/eprint/13325/>

**Link to published version:** <https://doi.org/10.1016/j.applthermaleng.2012.03.032>

**Copyright:** City Research Online aims to make research outputs of City, University of London available to a wider audience. Copyright and Moral Rights remain with the author(s) and/or copyright holders. URLs from City Research Online may be freely distributed and linked to.

**Reuse:** Copies of full items can be used for personal research or study, educational, or not-for-profit purposes without prior permission or charge. Provided that the authors, title and full bibliographic details are credited, a hyperlink and/or URL is given for the original metadata page and the content is not changed in any way.

---

---

---

City Research Online:

<http://openaccess.city.ac.uk/>

[publications@city.ac.uk](mailto:publications@city.ac.uk)

---

# The effects of thermistor linearization techniques on the T-history characterization of phase change materials

Stanislava B. Stanković\*, Panayiotis A. Kyriacou

School of Engineering and Mathematical Sciences, City University London, Northampton Square, London EC1V 0HB, UK

## A B S T R A C T

Phase Change Materials (PCMs) are increasingly being used in the area of energy sustainability. Thermal characterization is a prerequisite for any reliable utilization of these materials. Current characterization methods including the well-known T-history method depend on accurate temperature measurements. This paper investigates the impact of different thermistor linearization techniques on the temperature uncertainty in the T-history characterization of PCMs. Thermistor sensors and two linearization techniques were evaluated in terms of achievable temperature accuracy through consideration of both, non-linearity and self-heating errors. T-history measurements of RT21 (RUBITHERM® GmbH) PCM were performed. Temperature measurement results on the RT21 sample suggest that the Serial-Parallel Resistor (SPR)<sup>1</sup> linearization technique gives better uncertainty (less than  $\pm 0.1$  °C) in comparison with the Wheatstone Bridge (WB)<sup>1</sup> technique (up to  $\pm 1.5$  °C). These results may considerably influence the usability of latent heat storage density of PCMs in the certain temperature range. They could also provide a solid base for the development of a T-history measuring device.

## Keywords:

Thermistor  
Linearization technique  
PCM  
T-history method  
Temperature accuracy  
Heat density

## 1. Introduction

In the past few years the utilization of Phase Change Materials (PCMs) in applications for reduction of energy consumption and CO<sub>2</sub> emission has grown significantly [1]. Thermal characterization of these materials is essential prior to any application. Namely, according to Mehling and Cabeza [1] the commercial TES systems using PCMs as well as the heat transfer models involving phase change lack the experimentally determined material data, especially in terms of the heat release/storage density variation with temperature. Additionally, the accuracy of the reported results is questionable due to variant reports by different researchers as also indicated by Mehling and Cabeza [1]. This is one of the main limiting factors for the effective applications of PCMs.

Differential Scanning Calorimeter (DSC) and T-history are the two most commonly used methods for the investigation of thermo-physical properties of PCMs, as indicated in the comprehensive reviews written by Zalba et al. [2] and Zhou et al. [3] as well as in the research conducted by Castellon et al. [4], Zuo et al. [5], Cheng et al. [6] and Yinping et al. [7]. The DSC method has significant drawbacks mainly in terms of the limited sample size [7], possible

temperature gradient that can be created inside the sample [4], and relatively low signal to noise ratios [1]. The small sample size in DSC tests which results in higher degree of subcooling and lower degree of phase segregation [7] is the reason T-history was used in this study.

PCMs are able to store/release large amounts of heat in a narrow temperature range of few degrees. Günther et al. [8] reported that the typical temperature ranges of PCM applications are in the order of  $\pm 10$  °C around the phase change temperature of the material. Nevertheless, this range in practice is sometimes reduced to  $\pm 5$  °C or less (e.g. in free cooling applications) implying that the maximum decrease in the temperature uncertainty associated with the measurements on the PCMs is very important since it could provide a more optimal usage of these materials. The decrease in uncertainty can be achieved through the application of accurate temperature sensors during T-history measurements. In addition to temperature accuracy, the size of the sensor should be kept small enough in order to reduce any interference during the phase change process. The cause of such interference is due to the physical presence of the temperature sensor inside the PCM sample which can act as a nucleating agent and thereby change the natural course of the phase change process resulting in incorrect determination of PCM properties (e.g. the degree of subcooling) [1].

The majority of the T-history studies reported in the literature has not emphasized either the accuracy of the applied sensors or any other relevant sensor selection criteria as reported in the

\* Corresponding author. Tel.: +44 (0) 20 7040 3878; fax: +44 (0) 20 7040 8568.  
E-mail address: stankovic.stanislava.1@city.ac.uk (S.B. Stanković).

<sup>1</sup> Serial-Parallel Resistor (SPR), Wheatstone Bridge (WB).

studies conducted by Yinping et al. [7], Günther et al. [8], Kravaritis et al. [9,10] and Moreno-Alvarez et al. [11]. Few studies reported by Marin et al. [12,13] and Lazaro et al. [14] identified the usage of thermocouples and Pt-100 resistance temperature sensors. However, thermocouples, despite their small size, have limitations in terms of their implicit tolerances that without any measurement system errors can go above 0.5 °C [15]. The Pt-100 resistance temperature detectors are better than thermocouples, but their disadvantages are relatively low sensitivity and long response time [15]. Hence, thermistors have been used for temperature measurements in this T-history implementation.

Thermistors have very high sensitivity, making them particularly responsive to changes in temperature. Additional advantages are accessibility of small probes and short response time [22]. The main disadvantage of these sensors is the nonlinear change of their resistance with respect to temperature [16]. This requires the application of linearization technique. Various hardware linearization techniques have been developed over the years based on voltage divider or bridge circuits as reported by Tsai et al. [17], 555 timers as reported by Nenova and Nenov [18], as well as different software solutions as indicated by Khan et al. [19]. However, there is no reported documentation on the utilization and evaluation of these linearization techniques for the T-history PCM characterization. Therefore in this study, two hardware linearization techniques, one based on the Wheatstone Bridge (WB) configuration and the other, based on simple Serial–Parallel Resistor (SPR) circuit, are evaluated in terms of achievable temperature accuracy. MATLAB® models were implemented for both linearizing configurations in order to determine the optimal circuit parameters. Subsequently, those parameters were used for the circuit development. The calibration and the T-history measurements on RT21 PCM (RUBITHERM® GmbH [23]) were performed with both, the WB and the SPR circuits. Finally, experimental results were analyzed and compared to determine the effects of thermistor linearization techniques on the T-history characterization of PCMs and consequently on the usability of these materials.

## 2. Materials and methods

### 2.1. Temperature sensors

Thermistors were selected for this study due to their two main properties: high sensitivity and size. A negative temperature coefficient (NTC) MA100BF103A thermistor model with a sensitivity of 5%/°C and a 0.762 mm diameter probe was used [24]. The temperature dependence of the thermistor resistance  $R_t$  is given by the table of resistances with the nominal resistance of 10 kΩ at 25 °C. Its operating range is from 0 °C to 50 °C.

### 2.2. Linearization circuits

The principle of the linearization circuit is to transform the nonlinear thermistor's resistance–temperature change into a linear voltage–temperature dependency. The accuracy of such transformation depends on many factors including, the circuit itself, the circuit component values, and the linearizing temperature range. In this case the range was fixed between 10 °C and 39 °C to meet the application requirements [25], so the accurate temperature measurements had to be secured through the development of proper circuits with optimal component values. As noted in the introductory section two different circuits, the WB and the SPR were developed. The determination of optimal component values for these circuits was established through the implementation of MATLAB® linearization models which are explained in detail in Section 3.

#### 2.2.1. The WB thermistor linearization circuit

A circuit that is commonly used for thermistor linearization is based on the WB (Fig. 1).

The *OUTPUT* voltage of the WB circuit is given by Eq. (1):

$$OUTPUT = V_a - V_b \quad (1)$$

In order to stabilize the output of the bridge itself a differential amplifier is used. This was achieved through the utilization of three single operational amplifiers. The values for the resistor elements  $R_4$ ,  $R_f$ ,  $R_5$ , and  $R_g$  were selected in such way that the gain of the differential amplifier equals one and therefore the *OUTPUT* of the entire circuit equals the output voltage of the bridge. This *OUTPUT* is a single-ended voltage which is more suitable for the data acquisition systems, especially in cases of multiple channel measurements. Since the T-history implementation requires the measurement of at least three different temperatures (environmental, that of the PCM, and that of the reference material) this solution is feasible. The IC OP497FP was used for the implementation of the differential amplifier. The resistance values for resistor elements  $R_1$ ,  $R_2$ , and  $R_3$  were selected to be the same as the ones from the output of the corresponding MATLAB® model for this circuit.

#### 2.2.2. The SPR thermistor linearization circuit

The SPR linearization circuit, shown in Fig. 2, is simpler than the WB circuit. In this circuit the input voltage  $V_{CC}$  is divided between the resistor  $R_1$  and the parallel connection of the resistor  $R_2$  and the NTC thermistor. The output of the SPR connection is the voltage across the parallel resistor connection. A simple voltage follower is used to provide stable, single-ended voltage *OUTPUT*. The voltage follower is implemented with a single operational amplifier from the IC OP497FP. The determination of resistance values for  $R_1$  and  $R_2$  is explained in Section 3.

### 2.3. Calibration protocol

Prior to PCM T-history measurements proper sensor calibration with both linearization circuits was performed in a temperature controlled chamber (model BINDER KMF 115 [26]). Each sensor (three different ones) was subjected to 1 °C step temperature program from 10 °C to 39 °C. Recorded *OUTPUT* voltage data were evaluated at known temperatures (10–39 °C in 1 °C step) and the calibration curves and equations were determined using the least squares method for data fitting. The calculation of absolute errors between expected and fitted measured temperature data was performed and the obtained results are presented in Subsection 4.2.

### 2.4. T-history experimental protocol

T-history measurements of RT21 PCM were carried out in a temperature controlled chamber. The PCM sample and distilled water, used as reference, were subjected to a sharp temperature change between 30 °C and 11 °C and their temperature history recorded along with the environmental temperature. Firstly, measurements with sensors placed inside the samples were performed using both linearization circuits. Secondly, measurements with sensors placed on the surface of the samples' test tubes were also performed, but only using the SPR circuit. Data acquisition was performed utilizing a 14-bit NI DAQ USB 6212 card at a sampling frequency of 10 Hz [22]. Temperature values from the measured voltage data were calculated based on the equations obtained through linear fitting of voltage–temperature calibration curves using the least squares method. The temperature history data, obtained from the sensors placed inside the samples, were then

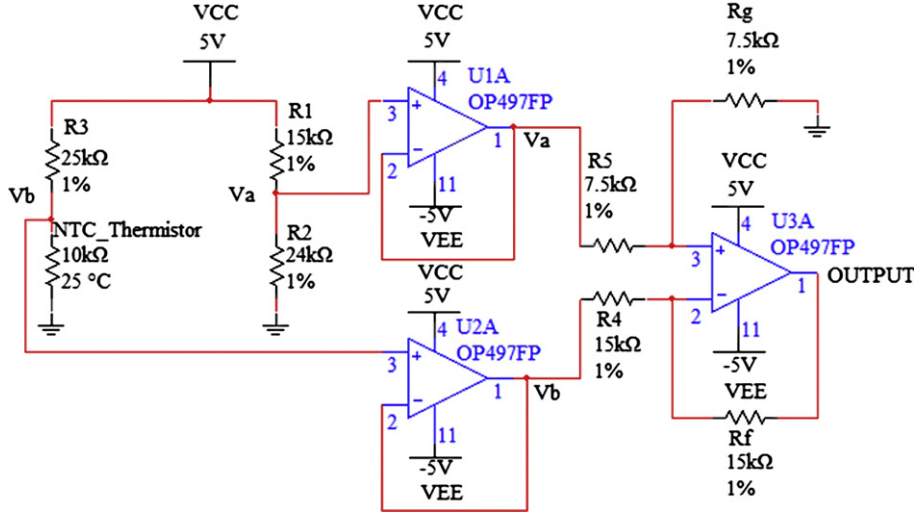


Fig. 1. The WB thermistor linearization circuit.

used for the determination of heat capacity of the investigated material RT21. The heat capacity was evaluated according to the mathematical model given by Marin et al. [12] and presented in form of heat density as the function of temperature in given temperature intervals as suggested by Mehling et al. [20].

### 3. Linearization models

Prior to the development of the linearization circuits the determination of the optimal components using MATLAB<sup>®</sup> linearization models was performed for each circuit. These models generate optimal component values providing fine linearization and accuracy through minimization of the thermistor's self-heating and non-linearity errors. Some restrictions for both models were defined. The first and stronger restriction was to keep the thermistor's self-heating error  $\Delta T$  below  $0.05^\circ\text{C}$  in order to keep the sensor from permanent damage. This error defines the value of the thermistor's maximum permissible current  $I_{\max}$  as indicated by Eq. (2):

$$I_{\max} = (\Delta TC/R_{t,\min})^{1/2} \quad (2)$$

where  $C$  denotes the thermistor's dissipation constant. Critical value (in air) of this constant for the selected thermistor is  $2.5 \times 10^{-3} \text{ W}/^\circ\text{C}$  [24].  $R_{t,\min}$  denotes the thermistor's minimal resistance in the operating temperature range. The thermistor's

maximum permissible current  $I_{\max}$  can be calculated as indicated by Eq. (2), as was done in this study, or it can be given as part of the thermistor's specification. This restriction can be expressed in the form of Eq. (3):

$$I_t < I_{\max} \quad (3)$$

where  $I_t$  denotes the thermistor's operating current. The second restriction was to minimize the non-linearity errors. This implies the linearization of the *OUTPUT* (see Figs. 1 and 2) voltage–temperature characteristic or otherwise known as the transfer function  $f(T)$ . The  $f(T)$  function is linear in a particular region if its second derivative with respect to temperature equals zero in that same region as shown in Eq. (4):

$$\partial^2 f(T)/\partial T^2 = 0 \quad (4)$$

Due to the rather complicated form of  $f(T)$  which includes at least two unknowns and one variable parameter  $R_t$ , in the case of both circuits the determination of the second derivative was not feasible, therefore a different numerical approach was used in the implementation of the models. Namely, the restriction of non-linearity error minimization was implemented through the determination of  $f(T)$  dependency for different combinations of circuit component values. Then the transfer function was fitted using the least square method and the optimal component values were determined based on the best linear fitting, i.e. the one that produced the minimal norm of the residuals. One additional restriction was to keep the supply voltage  $V_{CC}$  equal to the standard value of 5 V in order to minimize the circuit's power dissipation.

#### 3.1. Linearization model for the WB circuit

Since the WB is a form of a voltage divider the maximum permissible thermistor current  $I_{\max}$ , calculated from Eq. (2) or given as the part of sensor specifications, defines the value of resistor  $R_3$  as indicated by Eq. (5):

$$R_3 > V_{CC}/I_{\max} - R_{t,\min} \quad (5)$$

The application of the first restriction in this model produces an output indicating that  $R_3$  needs to be higher than 24.78 kΩ. This does not allow any flexibility for the reduction of non-linearity errors since the *OUTPUT* voltage is calculated by Eq. (1) and therefore determined by voltages  $V_a$  and  $V_b$  (see Fig. 1). The

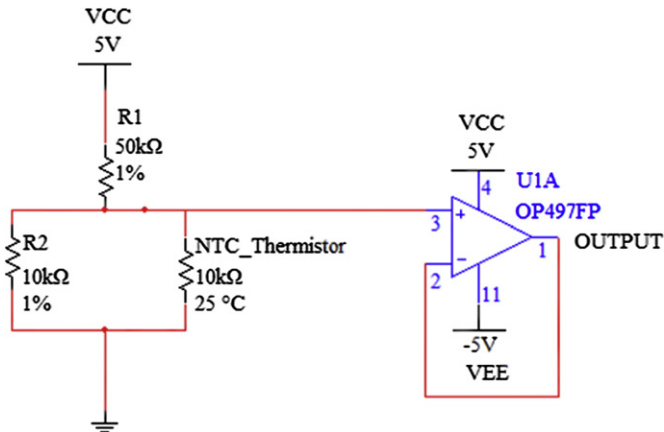


Fig. 2. The SPR thermistor linearization circuit.

restriction on  $R_3$  does not allow any flexibility for the minimization of non-linearity errors. The model shows that any higher resistance for  $R_3$  than the minimal value determined by Eq. (5) increases the non-linearity error i.e. the norm of residuals as explained above. Therefore the value of 25 k $\Omega$  was selected for the resistance  $R_3$ . This gave the fixed value for the voltage  $V_b$  and determined the shape of the transfer function  $f(T)$ . Further on, the only possible manipulation, modification of voltage  $V_a$ , was done in order to shift the *OUTPUT* (see Fig. 1) voltage to a range more suitable for measurements from 0.8 V to 2.2 V. This manipulation implemented in the model gave the values of 15 k $\Omega$  and 24 k $\Omega$  for  $R_1$  and  $R_2$ . The model showed that the circuit configuration is such that the minimization of self-heating error highly restricts the minimization of the non-linearity errors.

### 3.2. Linearization model for the SPR circuit

This model is more flexible since both restrictions, the self-heating and the non-linearity errors, can be considered simultaneously due to existence of two resistors which influence both the maximum permissible current  $I_{max}$  and the shape of the transfer function  $f(T)$ . As indicated at the start of this section the model was implemented through calculation of  $f(T)$  functions for different combination of resistor values  $R_1$  and  $R_2$ . The resistor values were changed in small steps of 20  $\Omega$  and then the calculated  $f(T)$  functions were fitted with linear polynomial functions using the least squares method. The best fitting function i.e. the one that gave the minimum norm of residuals was used to retrieve the optimal  $R_1$  and  $R_2$  values. The model gave the values of 53 k $\Omega$  and 8.89 k $\Omega$  for  $R_1$  and  $R_2$ . For the fixed value of resistance  $R_1$  the transfer function shows both linear and exponential behaviour in the same temperature range depending on the values of  $R_2$ . Fig. 3 shows that for an optimal value of  $R_1$  the output voltage–temperature dependency i.e. the transfer function shows relatively linear behaviour for the values of  $R_2$  below 20 k $\Omega$  (Fig. 3a). The best linearity is achieved for the optimal value of  $R_2$  as seen in Fig. 3b. Given the optimal values from the model the resistance values of 50 k $\Omega$  and 10 k $\Omega$  for  $R_1$  and  $R_2$  were chosen for the SPR circuit prototype.

## 4. Results and discussion

### 4.1. Absolute errors of the models

The *OUTPUT* (see Figs. 1 and 2) voltage–temperature dependency was calculated for both linearization circuits with optimal parameters. Calculations were performed for a temperature range between 10  $^{\circ}\text{C}$  and 39  $^{\circ}\text{C}$ . The linear polynomial fitting equations for the transfer functions were determined in the models as explained in Section 3 and then the absolute errors between real and fitted temperature values were calculated (see Fig. 4). As indicated in Fig. 4 linearization in the case of the WB configuration suggests maximum and mean errors of 1.69  $^{\circ}\text{C}$  and 0.67  $^{\circ}\text{C}$ . The errors for the SPR configuration are much smaller, with maximum and mean errors of 0.25  $^{\circ}\text{C}$  and 0.07  $^{\circ}\text{C}$ . In this case the greater errors appear only above 37  $^{\circ}\text{C}$  which is well beyond the required measurement range while the errors above the mean value in the WB configuration are distributed across the whole measurement range.

### 4.2. Absolute errors of the calibration measurements

As indicated in Figs. 5 and 6 calibration results for the two linearization circuits show good agreement with the model predictions. The results from the WB configuration show the mean and maximum error of 1.69  $^{\circ}\text{C}$  and 0.67  $^{\circ}\text{C}$  respectively which is in agreement with the model predictions, however unacceptable due

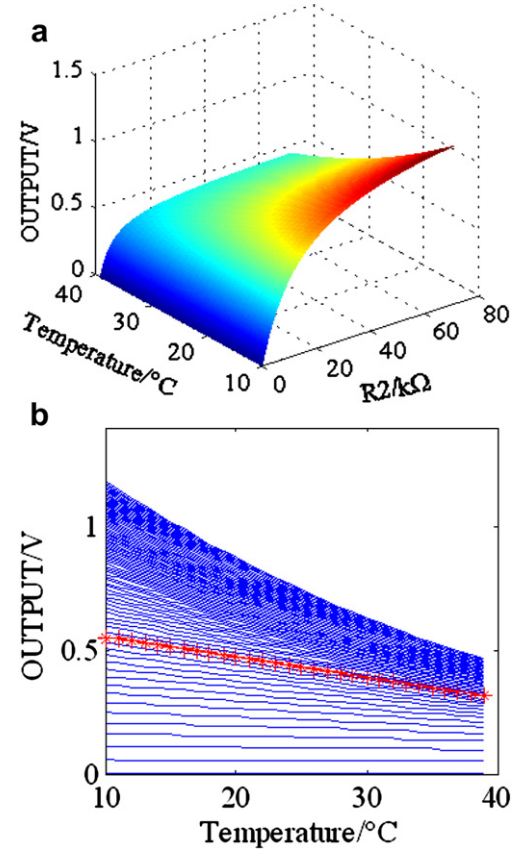


Fig. 3. The voltage–temperature dependencies i.e. the transform functions  $f(T)$  for optimal serial–parallel resistor circuit component value  $R_1 = 53$  k $\Omega$  and variable values of  $R_2$ . a) 3D view. b) 2D view with the optimal transform function for  $R_2 = 8.89$  k $\Omega$  shown in asterisk marked line.

to the error magnitude. In the case of the SPR configuration the values of 0.26  $^{\circ}\text{C}$  and 0.07  $^{\circ}\text{C}$  are recorded for the mean and maximum errors respectively. This is acceptable for the PCM temperature characterization especially due to the fact that for all three channels maximum errors occur above 30  $^{\circ}\text{C}$  – the highest temperature in T-history measurements.

### 4.3. T-history measurements

Firstly, T-history temperature measurements with sensors placed inside the samples were performed between 30  $^{\circ}\text{C}$  and

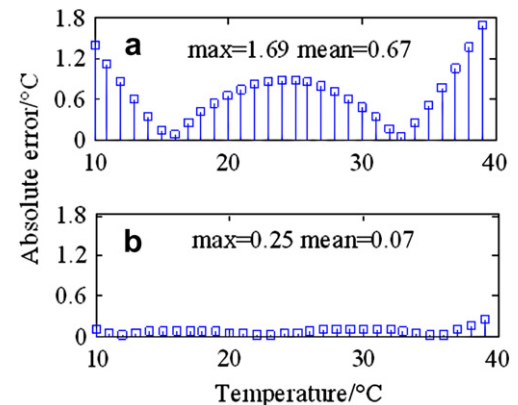
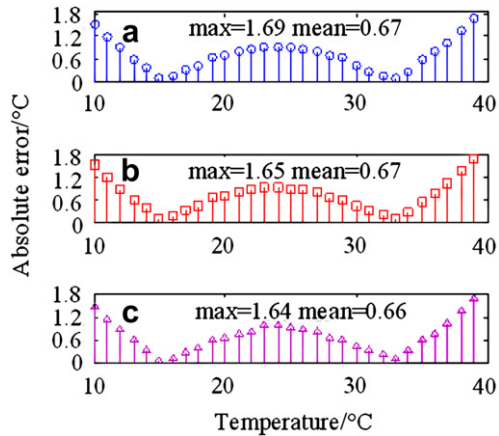
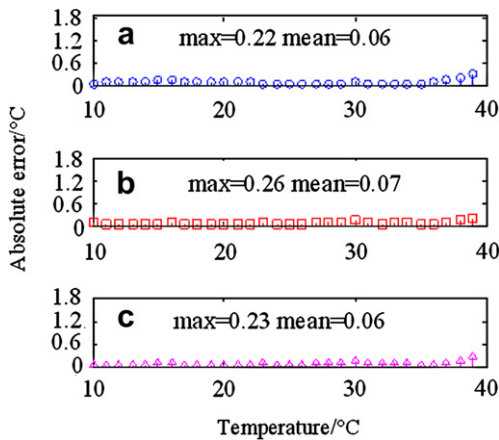


Fig. 4. Model predictions of absolute error values. a) The WB configuration. b) The SPR configuration.



**Fig. 5.** Calibration measurement based absolute error values for the WB configuration. a) Channel used for environment temperature measurement in the T-history implementation. b) Channel used for PCM temperature measurement. c) Channel used for water temperature measurement.

11 °C. Ten cooling cycles of the RT21 were recorded and the temperature results were averaged in order to minimize the random errors and improve measurement precision. Results obtained for the PCM temperature measurements through cycle averaging from the WB and from the SPR configurations are shown in Fig. 7. It can be seen that the PCM T-history curve obtained from the WB circuit during the first 10 min shows temperature higher than 30 °C which was the first equilibrium temperature in this investigation. On the other hand the T-history curve from the SPR circuit is sharply aligned with 30 °C (see Fig. 7). At the expected phase change temperature of 21 °C the SPR curve shows much better agreement than the WB curve which shows a deviation of up to 1 °C (see Fig. 7). The two curves intersect at 17.4 °C which is nearly the temperature at which calculated absolute errors for both, the WB model and the WB calibration measurements, reach minimum value (see Figs. 4a and 5). Therefore, it can be assumed that the difference between the WB and the SPR PCM cooling curves is due to the measurement accuracy of the corresponding linearization circuit and not due to the physical phenomena. Also, at the second expected equilibrium temperature of 11 °C the WB curve shows a deviation of 1.5 °C while the SPR curve shows a deviation of 0.1 °C.



**Fig. 6.** Calibration measurement based absolute error values for the SPR configuration. a) Channel used for environment temperature measurement in the T-history implementation. b) Channel used for PCM temperature measurement. c) Channel used for water temperature measurement.

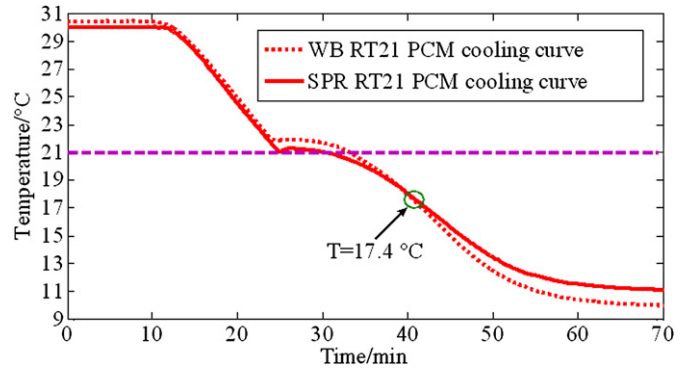


**Fig. 7.** Comparison of RT21 PCM T-history cooling curves. a) The WB configuration (dotted line). b) The SPR configuration (solid line).

Since the SPR technique showed better accuracy in the previous experiments, measurements with sensors placed on the surface of the test tubes were performed using only this technique. These measurements were performed under the same conditions as the measurements with the sensors inside the samples in order to compare the two. Ten cooling cycles of the RT21 were recorded and the results averaged to minimize errors. The results from surface measurements were compared with the results obtained from RT21 cooling with the sensor inside the sample as shown in Fig. 8. The RT21 cooling curve from the surface measurements shows the typical phase change temperature of 20.04 °C. This is around 1 °C lower than in the case of the interior temperature measurement which is in a good agreement with the typical phase change temperature of 21 °C. Maximum temperature deviation between the curves was 2.1 °C during the phase change while the curves are aligned at the equilibrium temperatures of 30 °C and 11 °C (see Fig. 8).

#### 4.4. Heat release density

Heat release density as the function of temperature in given temperature intervals during the RT21 PCM cooling was calculated from the interior measurement results of both, the WB and the SPR configurations (Fig. 9). The temperature precision in the calculations was 0.2 °C which is more precise than 1 °C reported by Mehling et al. [20]. Heat release density in the case of the WB configuration shows a peak value at 21.9 °C (see Fig. 9a). On the other hand the heat release density peak value in the case of the SPR configuration occurs at 21.1 °C which is in better agreement with the typical phase change temperature of 21 °C (see Fig. 9b).

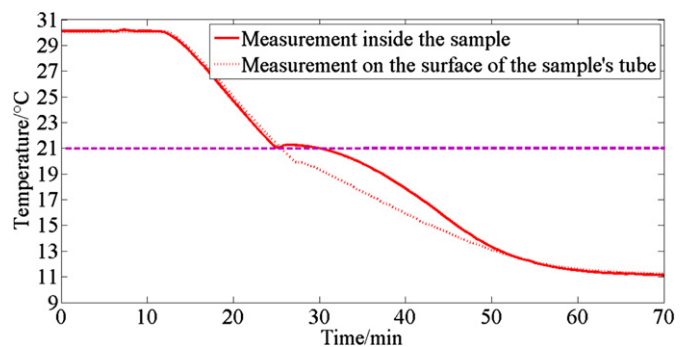


**Fig. 8.** Comparison of RT21 PCM T-history curves using the SPR configuration. a) Sensors placed inside the sample (solid line). b) Sensors placed on the surface of the sample's test tube (dotted line).

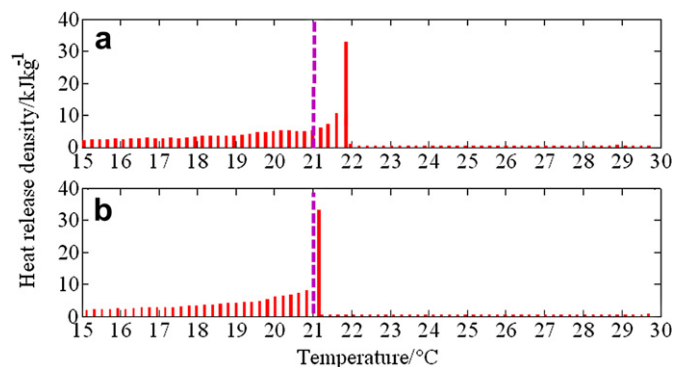


**Fig. 9.** Heat release density as the function of temperature in given temperature intervals during RT21 PCM cooling. a) The WB configuration. b) The SPR configuration.

## 5. Conclusion

Since PCMs store/release large amounts of heat in a narrow temperature range of a few degrees, accurate T-history measurements are of great importance. Temperature sensors need to be very sensitive in order to precisely detect temperature changes during T-history recording. Also, the sensors need to be small in order to minimize the interference with the natural course of the phase change process. Consequently thermistors have been selected for temperature measurements in this study due to their high sensitivity and miniature sizes. Further on, two hardware linearization techniques were compared in terms of achievable accuracy through minimization of both self-heating and non-linearity errors. The minimization of errors was achieved through the implementation of proper software models for each linearization circuit.

Both, model predictions and experimental results showed that lower absolute errors ( $\pm 0.1$  °C) were obtained by measurements performed when using the SPR configuration than with those performed with the WB configuration ( $\pm 1.5$  °C). The intersection temperature point of the WB and the SPR RT21 PCM cooling curves suggests that the difference between these curves is only due to the measurement accuracy of the corresponding linearization circuit and not due to the physical phenomena involved with the phase change process.

The comparison between the surface and interior temperature measurements on the RT21 sample, indicates that the measurements with sensors placed on the surface of the test tubes can lead to errors in PCM characterization. In order to investigate the last statement we compared our result to some reported in literature. Arkar and Medved [21] reported significant variation in the typical phase change temperature for the RT20 (former name of RT21 [23]) depending on the cooling rate used in their DSC tests. In case of 1 °C/min cooling rate (similar to 0.7 °C/min in our measurements) the typical phase change temperature reported by Arkar and Medved [21] was 19.7 °C. On the other hand, the same temperature reported by Kravvaritis et al. [10] from their T-history studies was around 21 °C, which agrees with the manufacturer's specifications [23]. Since the 19.7 °C is close to our surface measurement result of 20.04 °C, and 21 °C is similar to our interior measurement result of 21.1 °C we assume that the results of DSC tests significantly depend on the position of the temperature sensors inside the DSC instruments. Also, it can be concluded that the temperature measurements inside the samples during any PCM investigation could give more accurate results.

Finally, the analysis of the interior PCM cooling curves obtained with the WB and the SPR circuits resulted in 0.8 °C temperature shift of the peak values of the heat release density. This suggests that the selection of the linearization technique during material

characterization may affect the overall usability of PCMs, especially in applications where precise temperature control is important or where the PCM charging/discharging temperature range is narrow.

To conclude, the SPR thermistor linearization technique proved to be much better when used for PCM T-history investigation than the WB technique or the voltage divider. The main advantages in this approach are the reduced temperature uncertainty associated with the T-history characterization of PCMs and the simplicity of the electronic circuit. Since T-history implementation implies the utilization of at least three channels for the environmental, the PCM, and the reference temperature measurements, the compactness of the measuring circuit is desirable. Hence, the SPR linearization circuit may be very suitable for the implementation of a currently non-existent T-history commercial measuring device. Our results also show that sensor positioning in such a device would be significant. Moreover, the proposed SPR measurement system could provide the possibility for consistency in future T-history characterization studies of PCMs and easier comparison between the reported material data. The reported heat release density results, with low temperature uncertainty ( $\pm 0.1$  °C) and high temperature resolution (0.2 °C), could enable the development of better heat transfer models and therefore more reliable application of these materials in the commercial TES systems.

## Acknowledgements

The authors would like to express their gratitude to the Engineering and Physical Sciences Research Council (EPSRC) for the research funding and to the company RUBITHERM® GmbH [23] for providing the PCM samples.

## References

- [1] H. Mehling, L.F. Cabeza, *Heat and Cold Storage with PCM – An Up to Date Introduction into Basics and Applications*, Springer, Berlin, Germany, 2008.
- [2] B. Zalba, J.M. Marin, L.F. Cabeza, H. Mehling, Review on thermal energy storage with phase change: materials, heat transfer analysis and applications, *Appl. Therm. Eng.* 23 (2003) 251–283.
- [3] D. Zhou, C.Y. Zhao, Y. Tian, Review on thermal energy storage with phase change materials (PCMs) in building applications, *Appl. Energy* 92 (2012) 593–605.
- [4] C. Castellon, E. Günther, H. Mehling, S. Hiebler, L.F. Cabeza, Determination of the enthalpy of PCM as a function of temperature using a heat-flux DSC – a study of different measurement procedures and their accuracy, *Int. J. Energy Res.* 32 (2008) 1258–1265.
- [5] J. Zuo, W. Li, L. Weng, Thermal properties of lauric acid/1-tetradecanol binary system for energy storage, *Appl. Therm. Eng.* 31 (2011) 1352–1355.
- [6] W.-I. Cheng, N. Liu, W.-F. Wu, Studies on thermal properties and thermal control effectiveness of a new shape-stabilized phase change material with high thermal conductivity, *Appl. Therm. Eng.* 36 (2012) 345–352.
- [7] Z. Yinping, J. Yi, J. Yi, A simple method, the T-history method, of determining the heat of fusion, specific heat and thermal conductivity of phase change materials, *Meas. Sci. Technol.* 10 (1999) 201–205.
- [8] E. Günther, S. Hiebler, H. Mehling, R. Redlich, Enthalpy of phase change materials as a function of temperature: required accuracy and suitable measurement methods, *Int. J. Thermophys.* 30 (2009) 1257–1269.
- [9] E.D. Kravvaritis, K.A. Antonopoulos, C. Tzivanidis, Improvements to the measurement of the thermal properties of phase change materials, *Meas. Sci. Technol.* 21 (2010) 5103–5112.
- [10] E.D. Kravvaritis, K.A. Antonopoulos, C. Tzivanidis, Experimental determination of the effective thermal capacity function and other thermal properties for various phase change materials using the thermal delay method, *Appl. Energy* 88 (2011) 4459–4469.
- [11] L. Moreno-Alvarez, J.N. Herrera, C. Meneses-Fabian, A differential formulation of the T-history calorimetric method, *Meas. Sci. Technol.* 21 (2010) 7001–7005.
- [12] J.M. Marin, B. Zalba, L.F. Cabeza, H. Mehling, Determination of enthalpy–temperature curves of phase change materials with the temperature-history method: improvement to temperature dependent properties, *Meas. Sci. Technol.* 14 (2003) 184–189.
- [13] J.M. Marin, B. Zalba, A. Lazaro, New installation at the University of Zaragoza (Spain) of T-history method to measure the thermal properties, IEA ECES IA Annex 17 Advanced Thermal Energy Storage Techniques-Feasibility Studies and Demonstration Project 8th Workshop, 18–19 April 2005, Kizkalesi, Turkey, pp. 1–9.

- [14] A. Lázaro, E. Günther, H. Mehling, S. Hiebler, J.M. Marin, B. Zalba, Verification of a T-history installation to measure enthalpy versus temperature curves of phase change materials, *Meas. Sci. Technol.* 17 (2006) 2168–2174.
- [15] L. Michalski, K. Eckersdorf, J. Kucharski, J. McGhee, *Temperature Measurement*, second ed. John Wiley & Sons Ltd, Chichester, England, UK, 2001.
- [16] G. Rakocevic, Overview of sensors for wireless sensor networks, *Trans. Internet Res.* 5 (2009) 13–18.
- [17] C.F. Tsai, L.T. Li, C.H. Li, M.S. Young, Implementation of thermistor linearization using LabVIEW, in: *Proc. 5th Int. Conf. on Intelligent Information Hiding and Multimedia Signal Processing*, 12–14 September 2009, Kyoto, Japan, pp. 530–533.
- [18] Z.P. Nenova, T.G. Nenov, Linearization circuit of the thermistor connection, *IEEE Trans. Instr. Meas.* 58 (2009) 441–449.
- [19] S.A. Khan, D.T. Shahani, A.K. Agarwala, Sensor calibration and compensation using artificial neural network, *ISA Trans.* 42 (2002) 337–352.
- [20] H. Mehling, S. Hiebler, E. Günther, New method to evaluate the heat storage density in latent heat storage for arbitrary temperature ranges, *Appl. Therm. Eng.* 30 (2010) 2652–2657.
- [21] C. Arkar, S. Medved, Influence of accuracy of thermal property data of a phase change material on the result of a numerical model of a packed bed latent heat storage with spheres, *Thermochim. Acta* 438 (2005) 192–201.
- [22] National Instruments Corporation. Available from: <[www.ni.com](http://www.ni.com)> (last accessed on 17.01.12).
- [23] Rubitherm Technologies GmbH. Available from: <[www.rubitherm.com](http://www.rubitherm.com)> (last accessed on 17.01.12).
- [24] Newark/element 14. Available from: <[www.newark.com](http://www.newark.com)> (last accessed on 17.01.12).
- [25] Quality Association PCM e.V. Available from: <[www.pcm-ral.de](http://www.pcm-ral.de)> (last accessed on 17.01.12).
- [26] BINDER GmbH. Available from: <[www.binder-world.com/en](http://www.binder-world.com/en)> (last accessed on 17.01.12).